

Exploring the potential of barley husk polysaccharide, arabinoxylan in nanoparticle based drug delivery systems

Ume Ruqia Tulain^{1*}, Alia Erum¹, Nariman Shahid², Momina Usman¹,
Nadia Shamshad Malik³, Amina Riaz⁴, Ayesha Rashid⁴, Sana Sajjad¹

¹Faculty of Pharmacy, University of Sargodha, Pakistan, ²Faculty of Pharmacy, The University of Lahore, Lahore, Pakistan, ³Faculty of Pharmacy, Capital University of Science and Technology, Islamabad, Pakistan, ⁴Department of Pharmacy, Women University Multan, Pakistan

This study focuses on the extraction, characterization, and application of polysaccharide, Arabinoxylan (AX), derived from barley husk (*Hordeum vulgare*). Arabinoxylan was extracted by alkali extraction method with a significant yield of 26%. It was thoroughly characterized to ascertain its physicochemical properties such as percentage yield, solubility, swelling index, loss on drying, sulphated ash and micromeritics. Afterwards AX was employed as a polymer in the synthesis of controlled-release nanoparticles (NPs) of dexlansoprazole, an acid-labile drug. Ionic gelation and nanoprecipitation methods were employed to prepare various NP formulations, which were characterized using techniques such as zeta sizer, scanning electron microscopy (SEM), X-ray diffraction (XRD), Fourier-transform infrared spectroscopy (FTIR), and thermal analysis. FTIR confirmed the compatibility of nanoparticles while SEM results displayed that AX based nanoparticles were smooth and spherical in shape. Likewise, the thermal analysis revealed that nanoparticles were thermally stable. Furthermore, the AX-based nanoparticles demonstrated efficient entrapment efficiency of $79.59 \pm 4.6\%$ and $43.69 \pm 4.9\%$, along with sustained drug release profiles, following Korsmeyer-Peppas models. Ionic gelation method was observed to be comparatively better than nanoprecipitation method. Overall, this study showcases the potential of utilizing AX as cost-effective and renewable biomaterial for the development of polymer-based drug transport system, facilitating efficient and controlled drug delivery.

Key words: Biopolymer. Arabinoxylan. Controlled release. Nanoparticles.

INTRODUCTION

The recent advancements in drug delivery systems have driven the increasing use of safe, biocompatible, and biodegradable natural polymers. Among these, polysaccharides, particularly biopolymers, have garnered significant attention for formulating novel drug delivery systems such as matrix-controlled systems, microspheres, buccal films, nanoparticles, hydrogels, and fast disintegrating tablets. The term 'naturapolyceutics,' introduced by Gaur (2020) describes the utilization of

polymers of natural origin in the design of drug delivery systems (Ngwuluka, 2018). Polysaccharides exhibit noteworthy characteristics including biocompatibility, non-toxicity, biodegradability, economical availability, and ease of access, rendering them suitable excipients for drug delivery applications (Gaur *et al.*, 2020). Barley (*Hordeum vulgare*) husks, which are the by-products of grain crops, are rich in polysaccharides such as arabinoxylan (AX) and cellulose nanocrystals (CNCs). It contains cellulose (30-35%) and hemi-cellulose (30-33%). Various methods have been reported for the isolation of polysaccharides, with alkali extraction being the most widely employed. Arabinoxylans, the hemicellulose present in barley husks, possess arabino furanose and glucuronic acid moieties attached to a xylan backbone.

*Correspondence: U. R. Tulain. Faculty of Pharmacy. University of Sargodha. Sargodha, Pakistan. umeruqia.tulain@uos.edu.pk. ORCID: <https://orcid.org/00923316668588>

Moreover, Arabinoxylan possess a number of features such as emulsifier, viscosity enhancer, gel former etc. Leveraging their unique properties, particularly their ability to undergo swelling-deswelling transitions, AX has been extensively employed in fabricating various drug delivery systems including hydrogels, microspheres, nanoparticles, buccal films, and micelles (Li *et al.*, 2020; Morales *et al.*, 2021; Zaman, Hanif, Khan, 2018).

The development of suitable drug delivery systems is often hindered by challenges associated with drugs characterized by a short biological half-life or very high/low aqueous solubility (Wan *et al.*, 2019). High aqueous solubility can result in rapid and unpredictable drug release, while drugs with short half-lives require repeated administration to maintain optimal therapeutic concentrations (Desu, Pasam, Kotra, 2020). A wide range of formulations have been developed to overcome such issues. In this regard, nanoparticles have emerged as a preferred option over conventional dosage forms due to their ability to improve drug compliance, solubility, penetration, and further enable targeted, sustained, and controlled drug delivery (Deng *et al.*, 2020). Many natural and synthetic polymers are being used in the preparation of nanoparticle based formulations. Natural polymers are obtained from gums and mucilage of different origins like linseed, plantago seeds, wheat, barley etc. (Nagarajana *et al.*, 2015). This study aims to utilize AX to develop nanoparticles (NPs) for sustained drug release. AX extracted from *Hordeum vulgare* husks was used in the fabrication of nanoparticles.

Proton Pump Inhibitors (PPI's) belong to the acid labile class of drugs and are widely used in the management of peptic ulcer and gastro-esophagus reflux disease (GERD). PPI's include omeprazole, dexlansoprazole, lansoprazole and pantoprazole (Nasiri *et al.*, 2019). Peptic ulcer and GERD are both acid intolerant conditions and may become life threatening in geriatric patients. In GERD, the acid contents are refluxed back into the esophagus that results in mucosal damage and other painful symptoms in esophagus (Bredenoord, Pandolfino, Smout, 2013). Furthermore, GERD is a digestive disorder in which patient experiences sleep disorder and decreased

working ability (Fujiwara, Arakawa, Fass, 2013). The most effective treatment in GERD is acid suppression in GIT and for this reason, PPI's are widely used. Peptic ulcers develop in stomach lining, lower esophagus or small intestine as a result of inflammation caused by *H.pylori* (Dadfar, Edna, 2020).

Dexlansoprazole is a new generation PPI, R-enantiomer of lansoprazole. It is poorly soluble in water having a biological half-life of 1.5-2 hours. The drug is absorbed from GIT; hence it must be protected from acidic degradation in the stomach. To ensure this, the drug is marketed in the form of conventional enteric coated beads, hydrogels, multiple units, capsules, solid dispersions, microspheres and polymeric nanoparticles (Gulia *et al.*, 2023; Sontale *et al.*, 2020).

Henceforth, nanoparticles loaded with dexlansoprazole (DLP) were prepared using AX as a polymer. This formulation offers a novel approach for the delivery of acid-labile drugs, aiming to enhance palatability, patient compliance, and reduce dosing frequency. In summary, this research has been focused on extracting Arabinoxylan from barley husk and utilizing AX to develop innovative nanoparticle based drug delivery systems, with the goal of achieving sustained drug release. The potential applications of this system were demonstrated through the incorporation of a model drug, DLP, known for its solubility and half-life limitations, respectively. These findings could contribute to the advancement of drug delivery technology using natural polymers, enhancing the efficiency, compliance, and therapeutic outcomes of various medications.

MATERIAL AND METHODS

Material

Sodium chlorite, sodium dithionite, sodium hydroxide, hydrochloric acid, barium chloride, lactose, sulfuric acid, Tween 80, glacial acetic acid (GAA), and ethanol were purchased from Sigma Aldrich in Germany. Dexlansoprazole was obtained from Pharm Evo Pvt. Ltd. in Karachi, Pakistan, and Barley Husk was purchased from the local market. All the chemicals used were of analytical grade.

METHODS

Extraction of polysaccharide, Arabinoxylan

The extraction was conducted following previously reported method of alkali extraction with slight modification (Jajere, Achadu, 2017). A total of 100 g of barley husk was added to 1 L of 0.05 M HCl, and the resulting mixture was stirred for 16 h at room temperature. Subsequently, centrifugation was performed to recover the fiber. The recovered fiber was then mixed with 1 L of water, and the pH of the fiber suspension was adjusted to 4.0 using glacial acetic acid (GAA). Next, 22 g of sodium chlorite was added, and the extraction was carried out for 2 hours at a temperature of 75°C. After the specified time, the mixture was cooled, and the fiber was obtained through centrifugation and subsequently washed with water 15 times. The obtained fiber was stirred with a solution of 1 M NaOH containing sodium dithionite at room temperature for 16 hours to separate cellulose and hemicellulose. The extraction process was halted by adding hydrochloric acid (HCl), and the pH was adjusted to 7.0. This resulted in two phases: a water-soluble phase and an insoluble phase, which were separated by centrifugation. The insoluble phase, which was rich in cellulose, was washed with deionized water and separated. While, the water-soluble phase, containing hemicellulose, was added dropwise to double the volume of a 96% ethanol solution to precipitate hemicelluloses. The precipitated hemicellulose (Arabinoxylan) was separated by centrifugation and was further air-dried (Borjesson *et al.*, 2018).

Characterization of AX

Physicochemical characterization

The percentage yields of the AX were determined by dividing weight of extracted AX to the weight of barley husk as given in equation 1.

$$\text{Eq.1: Percentage yield (\% yield)} = \left[\frac{x}{y} \times 100 \right]$$

Where 'x' is the weight of AX and 'y' is the weight of barley husk (Moorthy *et al.*, 2017).

Solubility of AX was tested in different solvents including water, DMSO, ethanol, methanol, chloroform, sodium hydroxide and hydrochloric acid. For this purpose, 20 mg AX was added in 10 mL solvent and stirred for 16 hours. Then samples were centrifuged at 3000 rpm to separate insoluble portions. Each insoluble portion was dried to a constant weight and the amount was determined (Dhobale *et al.*, 2019).

To measure swelling index of AX, 1 g of biomaterial was added into measuring cylinder and volume occupied was observed. Then distilled water was added up to 100 mL and allowed to stand for 24 hours. After 24 hours, any increase in volume was observed. The swelling index was obtained using equation 2.

$$\text{Eq.2: Swelling index} = \frac{\text{Increase in volume}}{\text{Initial volume}} \times 100$$

To determine the loss on drying, the biomaterial was taken in porcelain dish and dried at 105°C under vacuum to constant weight. The loss on drying was determined by using equation 3.

$$\text{Eq.3: Loss on drying} = \frac{\text{Decrease in weight after drying}}{\text{Initial weight}} \times 100$$

The total ash content was determined by weighing and transferring 2 g of AX to tarred crucible which was placed in a graphite furnace. The temperature was steadily raised up to 675±25°C. The ash was collected and cooled in a desiccator. The weight of the ash of AX was measured and total ash content was determined by using equation 4 (Dhobale *et al.*, 2019).

$$\text{Eq.4: Total ash content} = \frac{\text{weight of ash}}{\text{weight of original sample}} \times 100$$

Finally, pH of the polymer solution was determined by preparing 1% aqueous dispersion of polymer. The probe of the digital pH meter was dipped in the dispersion and pH was noted once a constant value was obtained (Wikiera, Mika, Grabacka, 2015).

Micromeritics of extracted AX

Bulk density (ρ_b) was determined by weighing and sieving 100g of biomaterial followed by addition of powder in 250 mL graduated cylinder without compaction. The apparent volume (V_o) of powder was observed and ρ_b was calculated using equation 5.

$$\text{Eq.5: Bulk density } (\rho_b) = \frac{M}{V}$$

Where M is mass of AX and V is volume occupied by the AX.

Tapped density was determined by transferring the powder to a 250 mL glass cylinder and noting the apparent volume (V_o) of the powder without compaction. Then tapping was done for 500 times to observe tapped volume, V_a of the powder. Cylinder was tapped for further 750 times to determine the tapped volume, V_f . The V_f was considered as the final tapped volume. Tapped density of the powder was calculated by equation 6.

$$\text{Eq.6: Tapped density} = \frac{M}{V_f}$$

Where M is the mass of powder and V_f is the final tapped volume of powder (Gupta, Parvez, Sharma, 2015).

Compressibility index and Hausner's ratio of AX were calculated by putting relevant values in following formula.

$$\text{Eq.7: Compressibility index} = \frac{100(V_o - V_f)}{V_o}$$

$$\text{Eq.8: Hausner's ratio} = \frac{V_o}{V_f}$$

For determination of angle of repose of powder, a piece of paper was placed on the surface and a glass funnel was placed on the paper. Then powder was down

poured through funnel until heap of maximum cone height was obtained. Angle of repose of powder was determined using equation 9.

$$\text{Eq.9: } \tan \theta = \frac{H}{r}$$

Where "H" is height of the powder cone and r is radius of the powder cone (Bansal, Bajpai, 2020).

Formulation of AX based nanoparticles

Dexlansoprazole (DLP) loaded NPs, using AX as polymer were prepared by ionic gelation (FN1, FN2 & FN3) and nanoprecipitation methods (FN4, FN5 & FN6) as displayed in Table II. For FN1, FN2 & FN3, different amounts of AX were dissolved in distilled water and stirred for about 2 hrs at 70°C to prepare polymer solution. Drug was dissolved in ethanol and stirred for about 4 hrs to prepare drug solution (1% w/v) which was then added to polymer solution drop wise upon constant stirring. Solution of barium chloride (BaCl_2), as cross-linker or gelating agent was added drop wise until the colour of the solution changed and then further stirred for 1 hr for cross-linking. For other NP formulations, FN4, FN5 & FN6, few drops of tween-80 (2% v/v) as surfactant were mixed in distilled water. Drug solution (1% w/v) was prepared similarly by dissolving DLP in ethanol. Both were mixed to prepare organic phase. Afterwards, the aqueous phase (polymer solution) was prepared by the same method as mentioned above. Aqueous phase was added to organic phase drop wise until the colour changes to yellow or off white with constant stirring. Blank nanoparticles were also prepared following the same procedure except adding the drug solution. Later, all the formulations were ultracentrifuged at 16000 rpm for 30 minutes. Finally, the supernatant was separated and pellets were washed with distilled water several times and then air dried (Boddupalli, Ramani, Anisetti, 2019).

TABLE I - The compositions of AX based nanoparticles prepared by ionic gelation and nanoprecipitation method

Formulation code	Polymer AX(mg/mL)	Drug DLP(10mg/mL)	Cross-linker BaCl ₂ (mg/mL)
FN1	1	40	1
FN2	0.75	40	1
FN3	0.5	40	1
Formulation code	Polymer AX(mg/mL)	Drug DLP(10mg/mL)	Surfactant Tween-80 (%v/v)
FN4	1	40	0.2
FN5	0.75	40	0.2
FN6	0.5	40	0.2

Preliminary characterization of AX based nanoparticles

Particle size and zeta potential

Prepared polymeric nanoparticles were characterized for particle size, zeta potential and poly dispersity index (PDI) using Malvern zetasizer.

Entrapment efficiency (%EE)

The entrapment efficiency was calculated by taking difference in absorbance of the total compound and the free compound. The compound solution only is referred to as the total drug while free compound is the supernatant of the nanoparticles which remains untrapped after centrifugation at 12000rpm for 30 minutes. To determine %EE, dilutions of total compound and free compound were prepared in pH 7.4 phosphate buffer. By using UV-visible spectrophotometer, the absorbance was taken at 285nm and %EE was determined by the following equation (Boddupalli, Ramani, Anisetti, 2019).

$$\text{Eq.10: \%EE} = \frac{\text{Abs of total comp} - \text{Abs of free comp}}{\text{Abs of total comp}} \times 100$$

Instrumental analysis of nanoparticle formulations

All AX based nanoparticles formulations were characterized to analyse their morphology, structure as well as any interactions.

Fourier Transform Infra-Red Spectroscopy

Fourier Transform infrared (FTIR) spectroscopic analysis was performed for DLP, AX, blank and drug loaded NPs to analyse any interaction by FTIR spectrometer. Powdered samples were analysed by FTIR spectrophotometer setting the scanning range in the region 4000-400 cm⁻¹ and keeping resolution of 2 cm⁻¹ (Shahid *et al.*, 2022).

Scanning Electron Microscopy

Surface morphology of polymeric nanoparticle formulations was observed under scanning electron microscope ((FEI Quanta 250 TM FEG). The pellets of the formulation were dried that were obtained after centrifugation. The samples were prepared by sprinkling the nanoparticles on aluminum stub. The coat sputter was used to coat the stub with gold-palladium alloy by using double adhesive tape. The samples of nanoparticles were examined under SEM and photographs were taken (Raval *et al.*, 2019).

Thermal analysis

Thermogravimetric analysis (TGA) and Differential scanning calorimetry (DSC) studies of arabinoxylan, pure drug and polymeric nanoparticles were performed by using SDT Q-600. The integrity and identity of pure drug and nanoparticles formulations were analyzed by DSC and TGA studies. The air dried samples were scanned at 0-500°C temperature range with heating rate of 20°C/min and thermographs were obtained (Haseeb *et al.*, 2019).

In-vitro drug release studies

Dialysis tubing method was adopted to determine the *in-vitro* drug release profile of the polymeric NPs in pH 1.2 buffer for 2 hrs and pH 6.8 buffer for 24 hrs. Dried sample of 5mg was taken in a dialysis tubing (Mw cut off of 12kDa), immersed in respective buffer solutions maintained at 37°C ± 0.5 and continuously stirred at 100 rpm in USP dissolution apparatus II. 5mL samples were taken at 0, 0.5, 1, 2, 4, 8, 12 and 24 hrs, filtered, diluted and analysed by UV Spectrophotometer at 285 nm. Standard curves of DLP were prepared in pH 1.2 and 6.8 buffers (Tulain *et al.*, 2021).

Drug release kinetics of AX based nanoparticles

By using model dependent approach, drug release profile of dexlansoprazole from polymeric nanoparticles was evaluated. Various kinetic models such as first and zero order, Higuchi, Korsmeyer Peppas and Hixon-Crowell kinetic model were used to analyse dissolution profiles of DLP loaded nanoparticles by employing DD solver software (Erum *et al.*, 2022).

Statistical Analysis

All of the results were statistically analysed. Obtained results were stated as mean ± SD (Standard Deviation). Student T-test was applied on the Arabinoxylan nanoparticles formulations using DD solver software

RESULTS & DISCUSSION

Extraction and characterization of arabinoxylan

Arabinoxylan from the *Hordeum vulgare* (barley) husks was successfully extracted by alkali extraction method with the percentage yield of 26% w/w. It has been reported that the barley husks are comprised of more than one third (30 to 40%) of the hemicelluloses, primarily arabinoxylan. In addition, in the primary cell wall of cereals, many AXs along with other polymers are crosslinked with other cell wall components to constitute the water insoluble structural network. Hence, due to the presence of such crosslinks, a major part of AXs cannot be extracted easily (Roos *et al.*, 2009). The hydroxyl ions from alkali increase swelling of cellulose which promotes destruction of intermolecular hydrogen bonding. They also disrupt the ester linkages, carboxyl groups, acetyl groups and benzyl groups. The hydrolysis of these linkages causes solubilization of AX from insoluble cell matrix. The obtained high yield of 26% of AX was also due to delignification. The delignification of barley husks break bonds between lignin and AX by hydrolysing ester linkages thereby facilitating the extraction of AX (Ávila, Martins, Goldbeck, 2021). Furthermore, alkali imbibition preceding heat treatment constrains the arabinoxylan degradation. Impregnation with alkali was utilized to prevent acidic environments through steam pretreatment as an acidic condition along with high temperature can result in hydrolysing the glycosidic links of the xylan backbone in AX. Hence, on a total weight basis 26% was an efficient yield. Results of various characterization parameters for extracted AX are summarized in Table II.

TABLE II - Physicochemical properties of arabinoxylan

Parameters	Arabinoxylan
%age yield	26 %
Solubility	
Cold water	Poorly soluble
Hot water	Soluble
DMSO	Soluble

TABLE II - Physicochemical properties of arabinoxylan

Parameters	Arabinoxylan
Chloroform	Insoluble
Ethanol	Soluble
0.5M NaOH	Soluble
Ash content (%)	1.4
Loss on drying (%)	5.4
Swelling index (%)	4
pH	4.6

The solubility of AX depends on degree of substitution of β -xylan chain. The un-substituted xylan chains become relatively flexible and form hydrogen bonds with themselves or with other arabinoxylan molecules leading to self-aggregation and insolubility. However, the arabinosyl units attached to xylan chain impose steric hindrance which limits the aggregation. So, the solubility of AX was due to these highly substituted soluble counterparts (Shrestha *et al.*, 2019).

The low values of swelling index suggest that these biomaterials can be used for controlled delivery of drugs. Furthermore, the ash content and loss on drying of AX were within the limits of US Pharmacopoeia. The lower value of ash content was due to the strong alkali and acid treatments. Loss on drying is an important parameter because biomaterials with less value can be used for hygroscopic drugs.

Micromeritic properties of AX

The flow properties of AX are given in Table III. The values of Hausner's ratio, compressibility index and angle of repose for AX indicated poor flow properties. A low value of angle of repose (25° - 30°) suggests excellent flow but a high value ($>45^{\circ}$) suggest a poor flow. Hence an angle of repose of 47° suggest poor flow of AX. It was also reported in previous studies that AX being polymeric in nature, exhibit poor flow properties (Zaman, Hanif, Sultana, 2018).

TABLE III - Micromeritic properties of arabinoxylan

Properties	Arabinoxylan
Bulk density (mg/mL)	0.026
Tapped density (mg/mL)	0.037
Hausner's ratio	1.41
Compressibility index (%)	28.9
Angle of repose (θ)	47

Preliminary characterization of AX based nanoparticles

AX based nanoparticle formulations were successfully fabricated having an average particle size in the range of 556.8-864.5nm and average diameter of 709.0nm. The results displaying a comparative evaluation of Z-average (d.nm), polydispersity index (PDI), zeta potential and entrapment efficiency (%) of various nanoparticle formulations have been presented in Table IV. It is evident from the results that by decreasing the concentration of polymer(AX), Z-average is markedly decreased by both ionic gelation and nanoprecipitation method. The prepared nanoparticles showed mean diameter of 763.6nm by ionic gelation method and 654.3nm by nanoprecipitation method. Hence, nanoparticles produced by nanoprecipitation method demonstrated reduced particle size as compared to those produced by ionic gelation method. Figure 1 displays the particle size distribution of various NP formulations. It was previously reported that size of nanoparticles was increased by increasing the concentration of polymer (Sharma, Madan, Lin, 2016). Likewise, the Zeta potential was found to be in the range of -29.9mV to -18.1mV. The negative values of zeta potential were due to the surface charge density produced by stearic hindrance and due to the presence of ionized carboxyl-groups. This proved the stability of the NPs due to the presence of repulsive forces which prevent their coalescence. The values of zeta potential by ionic gelation were comparatively better than nanoprecipitation method. All the six formulations (FN1 to FN6) showed good polydispersibility index (<0.45). This indicates the monodisperse system of fabricated nanoparticles (Haseeb *et al.*, 2019).

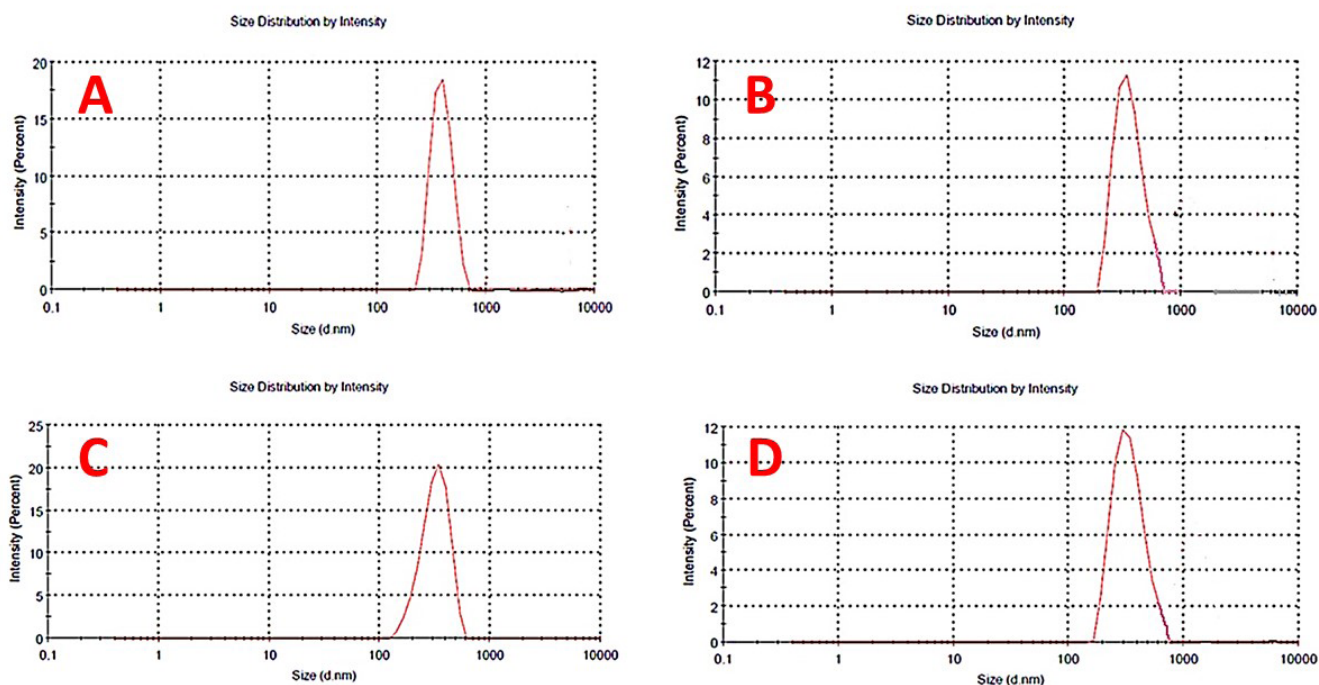


FIGURE 1 - Particle size distribution of AX based nanoparticle formulations, FN1 (A), FN2 (B), FN5 (C) and FN6 (D).

Similarly, entrapment efficiency of the NPs increased as the concentration of the polymer increased due to greater linkage area. EE for all the formulations by both ionic gelation and nanoprecipitation method was in the range of $79.59 \pm 4.6\%$ to $43.69 \pm 4.9\%$ as shown in the Table IV. The results displayed that the nanoparticle formulations prepared by ionic

gelation method demonstrated efficient entrapment efficiency as compared to the formulations prepared by nanoprecipitation method. Herein, FN1 displayed maximum EE of 79.59% , while FN6 displayed minimum EE of 43.69% among all formulations. These results were found comparable to those of previously reported (Nagarajana *et al.*, 2015).

TABLE IV - Comparative evaluation of AX based nanoparticle formulations*

Formulations	Z-average (d.nm)	PDI	Zeta potential (mV)	Entrapment efficiency (%)
FN1	864.5 ± 4.7	0.39 ± 0.02	-29.9 ± 3.9	79.59 ± 4.6
FN2	744.3 ± 5.6	0.35 ± 0.04	-28.3 ± 4.1	62.72 ± 3.6
FN3	682.2 ± 4.5	0.25 ± 0.03	-27.1 ± 3.6	59.98 ± 4.5
FN4	820.1 ± 4.6	0.21 ± 0.03	-28.3 ± 4.6	63.76 ± 3.8
FN5	586.2 ± 5.2	0.19 ± 0.02	-26.7 ± 3.8	58.69 ± 3.2
FN6	556.8 ± 3.9	0.15 ± 0.02	-18.1 ± 3.4	± 4.9

* Data represented as mean \pm SD, n=3

Instrumental analysis of nanoparticle formulations

Fourier Transform Infra-Red Spectroscopy

FTIR spectrum of Barley Husk AX showed a broad band at 3379.05 cm^{-1} and 3119.24 cm^{-1} in Figure 2A, which was due to the OH stretching vibrations reflecting the presence of intra/inter- hydrogen bonding in the polysaccharide network. The peak at 2973.66 cm^{-1} indicated the asymmetric stretching vibrations of CH₂ group. The finger-print region of polysaccharide was observed at $1200\text{--}800\text{ cm}^{-1}$ containing multiple peaks attributed to the vibrations of C-C-O, C-OH, and C-O-C. Amid the finger-print zone, the region from $1200\text{--}1000\text{ cm}^{-1}$ arises due to vibrations of overlapping of ring with glycosidic linkages and lateral groups. The high intensity band at 897.87 cm^{-1} presented the glycosidic linkages present between different sugar units which indicated the presence of xylose units are linked by β -linkages. The presence of low intensity

peaks at 982.88 cm^{-1} and 1164.97 cm^{-1} is indicative of arabinosyl units which is characteristic of AX type hemicelluloses (Guo *et al.*, 2019).

Figure 2B presented the FTIR spectra of dexlansoprazole. The peak at the frequency of 3096.56 cm^{-1} indicated C-H stretching in hetero aromatic ring, peak at 1460.90 cm^{-1} showed C-C stretching of phenyl ring, peak at 3449.61 cm^{-1} indicated N-H stretching in heterocyclic ring, peaks at 1036.59 cm^{-1} , 1110.13 cm^{-1} and 616.45 cm^{-1} indicated S=O, C-F and C-S stretching (Ganesh *et al.*, 2016). Furthermore, the FTIR spectra of unloaded AX nanoparticles demonstrated major peaks at frequencies of 3307.36 cm^{-1} , 1645.32 cm^{-1} , 1255.97 cm^{-1} and 1041.40 cm^{-1} indicating the presence of OH, COO-, COH and COC groups, respectively. The presence of Tween-80 was marked by the stretching peaks of C=C at the frequency of 1574.66 cm^{-1} and C-C at 888.96 cm^{-1} . This revealed that Tween-80 has got embedded in arabinoxylan and resulted in the formation of nanoparticles (Khan *et al.*, 2011).

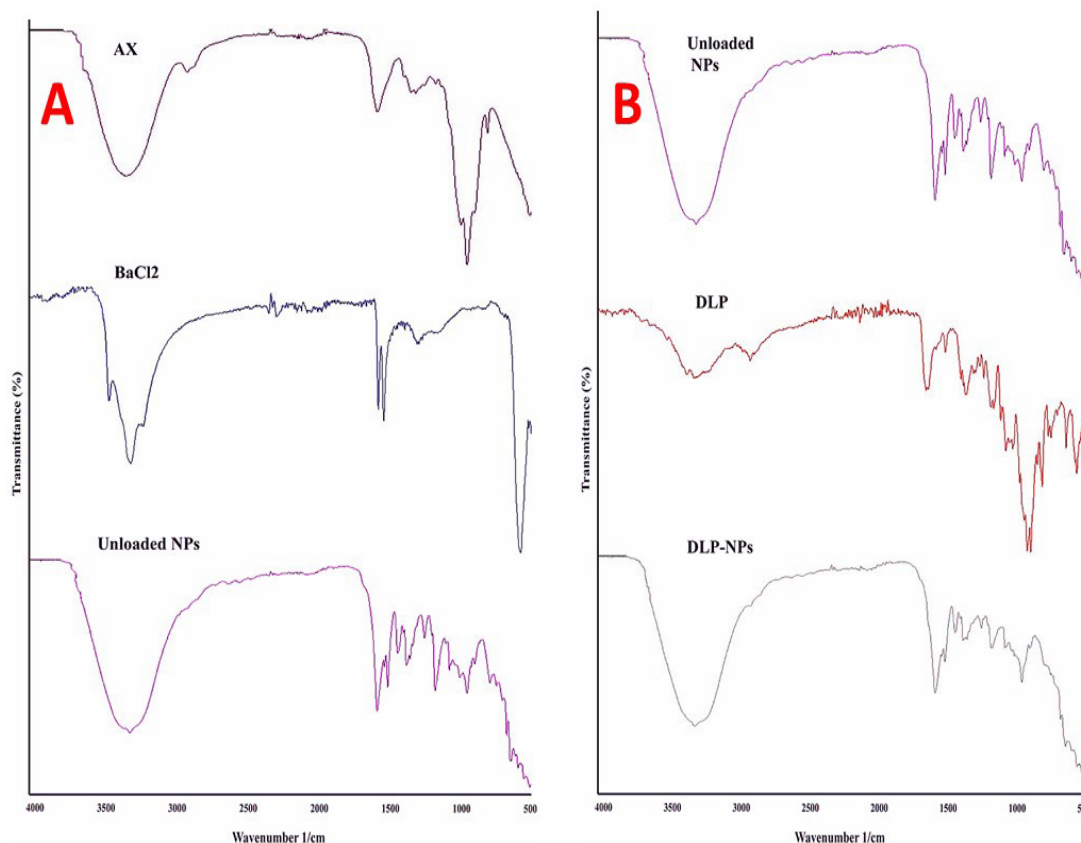


FIGURE 2 - FTIR overlay of AX, BaCl₂ and unloaded NPs (A); unloaded NPs, DLP and DLP-Loaded NPs (B).

All the peaks present in DLP were also observed in DPL loaded NPs indicating efficient drug loading. The major stretching peaks at the frequencies of 3335.86cm^{-1} , 2983.66cm^{-1} , 1636.77cm^{-1} , 1397.95cm^{-1} reflected the presence of OH, CH₂ and COO- groups respectively in both preparations. This indicated the presence of AX in the formulation while peaks observed at 3096.56cm^{-1} indicated C-H stretching in hetero aromatic ring, peak at 1470.90cm^{-1} showed C-C stretching of phenyl ring, peak at 3449.61cm^{-1} indicated N-H stretching in heterocyclic ring, while peaks at 1046.59cm^{-1} , 1110.13cm^{-1} and 616.45cm^{-1} indicated S=O, C-F and C-S stretching. Furthermore, the frequency band at 1574.66cm^{-1} and 888.96cm^{-1} indicated presence of Tween-80 while the spectral peaks observed at 3308.21cm^{-1} and 1599.57cm^{-1} indicated the presence of barium chloride (Erum *et al.*, 2023).

Scanning electron microscopy (SEM)

The photographic representation of morphological analysis of AX based nanoparticles by SEM is given in Figure 3 (A & B). The SEM micrographs revealed that NPs of optimized formulations displayed a spherical and smooth morphology as represented by small clusters. Micrographs of the arabinosylian based nanoparticles showed that nanoparticles of FN1 were spherical and smooth in shape while FN4 were irregular in shape. Images were taken at different resolutions (100x, 500x and 1000x). These images evidence the formation of nanoparticles (Shahid *et al.*, 2022).

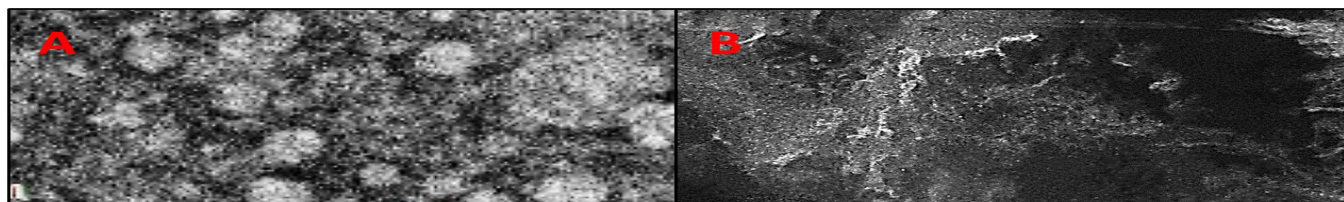


FIGURE 3 - SEM image of DLP loaded nanoparticles FN1 at Potential Energy of 2.9 Kv, magnification of 100x (A) and FN4 at magnification of 1000x (B).

Thermal analysis

Thermal analysis was carried out and comparative TGA and DSC thermograms of AX, unloaded NPs, DLP and DLP loaded NPs are shown in Figure 4 (A, B, C & D). The thermal stability of AX depends on its arabinose content. The higher content of arabinose required higher degradation temperatures (Borjesson *et al.*, 2018). Figure 4A represent the TGA curves of AX and unloaded NPs while 4B represent those of drug and DLP loaded NPs. TGA curve of arabinosylian presented 13.02% initial weight loss at 200°C after 3.55 min and then presented the gradual weight loss. At 300°C , weight loss was 36.42% and at 400°C it was 48.28%. TGA curve of unloaded NPs, the initial weight loss was 5.32% approximately at 100°C and at 400°C mass left was 65.25%. AX showed three stages of thermal degradation (Figure 4A). The first

degradation was observed at 70.5°C with initial small weight loss corresponding to the evaporation of absorbed water. The onset degradation temperature (T_{onset}) for second degradation was observed at 215°C . The second degradation was due to the decomposition of polymer chains into high mass volatile components resulted in weight loss of 36%. Third stage of thermal degradation at 365°C was due to complete breakdown of AX into gaseous (Ali *et al.*, 2017).

Moreover, TGA curve of DLP loaded NPs showed the initial weight loss of 5.32% at 100°C and 68.33% mass left at 400°C . Initial weight loss indicated the moisture content at various temperatures. Figure 4A indicated that unloaded NPs are more stable than pure AX because the mass left of arabinosylian was greater than even on higher temperature. Similarly, Figure 4B revealed that DLP loaded NPs were more stable than both unloaded NPs

and pure drug (DLP) due to comparatively lesser weight loss even at higher temperatures (Gaspar *et al.*, 2016).

The glass transition temperature of formulations and individual ingredients were also measured through calorimetry. The initial endothermic peaks indicated moisture loss followed by melting peaks while exothermic peaks displayed thermal degradation. In DSC thermographs as shown in Figure 4 (C & D), endothermic peaks of AX, unloaded NPs, DLP and DLP loaded NPs

were observed around 80°C, 117°C, 139°C and 109°C while exothermic peaks were observed at 475°C, 275°C, 397°C and 230°C, respectively (Gaspar *et al.*, 2016). It has been reported that DLP displays endothermic peak near 140°C representing its melting point. Dexlansoprazole was probably transformed from its crystalline towards amorphous form during the production course as the drug dispersed in the polymer matrix, as demonstrated by substantial reduction in the melting point of DLP.

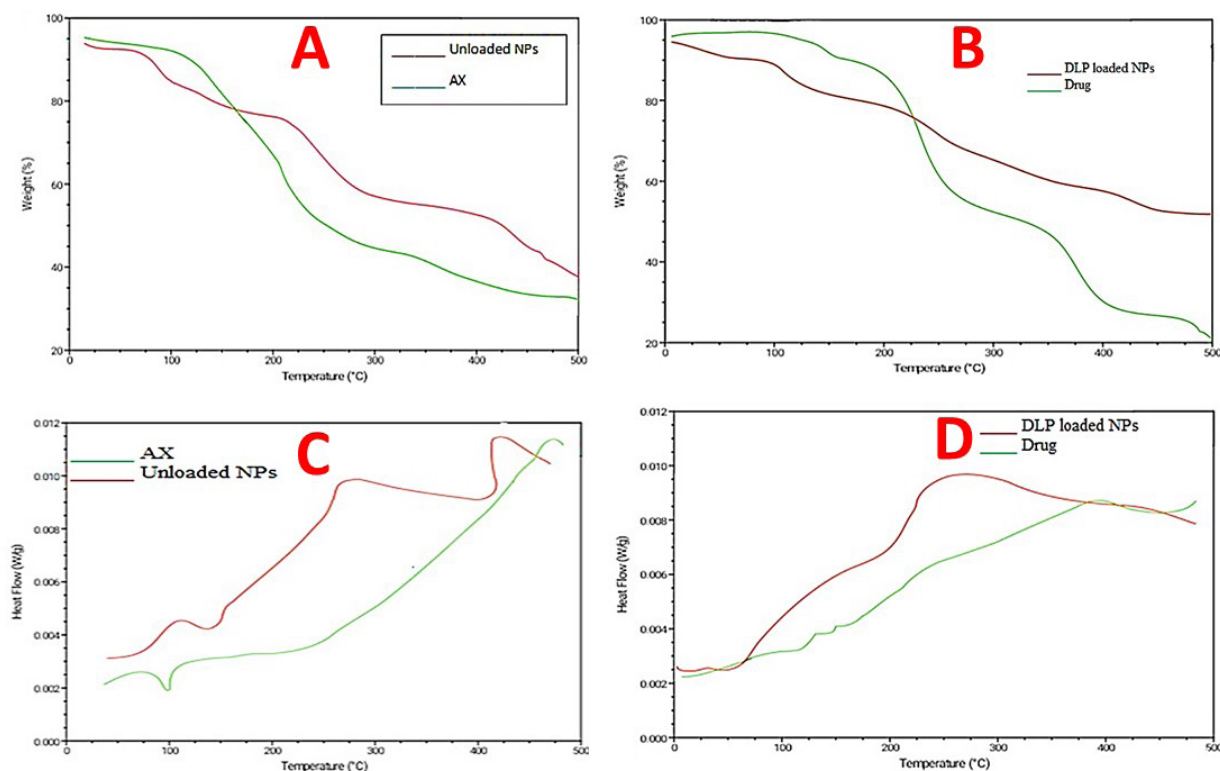


FIGURE 4 - TGA curves of AX and Unloaded NPs (A), DLP and DLP loaded NPs (B); DSC curves of AX and unloaded NPs (C) & DLP and DLP loaded NPs (D).

In-vitro drug release studies

The graphical representation of *in-vitro* drug release study of DLP loaded NPs is presented in Figure 5. *In-vitro* drug release studies demonstrated that all NP formulations showed a gradual and slow release at start due to the acidic medium. During first 2 hours, drug release was about 5.66-9.44% by both methods. Whereas, the drug release in basic medium with pH 6.8 was greater but in a controlled, slow and sustained manner. The

sustained drug release pattern can be attributed to the nature of the AX utilized as a polymer. Percentage release of formulations prepared by Ionic gelation method (FN1, FN2, FN3) was in range of 67.53 – 82.55 percent and for formulations prepared by Nanoprecipitation method (FN4, FN5, FN6) was in the range of 60.55 – 78.58 percent in alkaline medium. This showed the sustainability of NPs at basic pH that gradually increased with time due to drug diffusion. Henceforth, based upon the results, the ionic gelation method exhibited better drug loading and drug

release profile as compared to nanoprecipitation method. Hence, the sustained drug release profiles displayed by

DLP loaded AX based NPs have been found compatible with the oral route of administration.

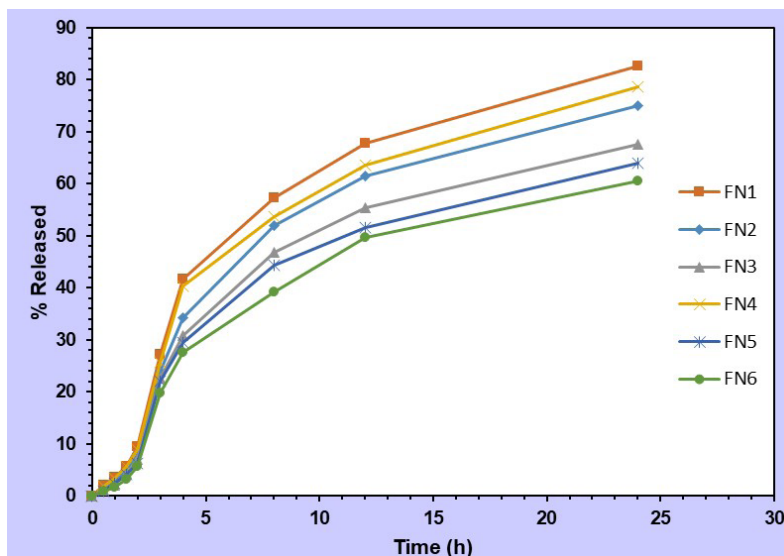


FIGURE 5 - Percentage release of DLP from DLP loaded NPs.

Drug release kinetics of AX based nanoparticles

Various kinetic models were employed to evaluate the drug release kinetics of AX based NPs. The values of R^2 showed that Korsmeyer-Peppas model best fit to regression equation as R^2 values of the Korsmeyer-Peppas were more and in the range of 0.991 to 0.997 (close to 1) than all other models. There are multiple release mechanisms involved in the drug release like erosion, chemical interactions between drug and

polymer, swelling of polymer matrix and diffusion. Correlation coefficient values have been tabulated in the Table V which confirms the drug release kinetics of various formulations prepared by ionic gelation and nanoprecipitation methods. Moreover, release exponent values (n) were established to be above 0.6 that proposed non-Fickian drug release mechanism. Furthermore, the extent of cross-linking of AX is an imperative factor in promoting drug release other than diffusion (Haseeb *et al.*, 2019).

TABLE V - Correlation co-efficient (R^2) & release exponent (n) of various kinetic models

Formulations	Zero-order	First-order	Higuchi	Hixon-Crowell	Korsmeyer-Peppas	
	R^2	R^2	R^2	R^2	R^2	n
FN1	0.762	0.960	0.887	0.943	0.991	0.617
FN2	0.786	0.957	0.887	0.933	0.997	0.634
FN3	0.783	0.941	0.885	0.910	0.994	0.633
FN4	0.764	0.954	0.888	0.930	0.992	0.617
FN5	0.780	0.931	0.885	0.898	0.984	0.630
FN6	0.801	0.931	0.882	0.902	0.988	0.648

Statistical analysis

Comparison between the two methods, Ionic gelation method (FN1, FN2, FN3) and Nanoprecipitation method (FN4, FN5, FN6) was done by using T-Test. Results of T-Test have been presented in the Table VI

and graphically represented in Figure 6. These results show insignificant differences between the two methods as the p value was greater than 0.05. Henceforth both methods have displayed comparable release profiles but the ionic gelation method displayed slightly better drug release profile as revealed in Figure 6 (Alai, 2014).

TABLE VI - Statistical Analysis of Ionic gelation and Nanoprecipitation method (T-test at each time point)

Time (h)	n-R	Mean R F (%)	SD-R	n-T	Mean-T F (%)	SD-T	Diff-Mean T-R	P-value
0.5	3	3.8680	0.7369	3	3.2104	0.8701	0.6576	0.3744
1	3	7.5827	1.4160	3	6.3127	1.6806	1.2700	0.3735
1.5	3	11.1504	2.0408	3	9.3107	2.4346	1.8397	0.3726
2	3	14.5771	2.6145	3	12.2081	3.1351	2.3690	0.3717
3	3	21.0298	3.6209	3	17.7150	4.3867	3.3148	0.3699
4	3	26.9837	4.4580	3	22.8602	5.4564	4.1235	0.3681
8	3	46.5537	6.4877	3	40.2960	8.2735	6.2576	0.3608
12	3	60.7827	7.0921	3	53.6436	9.4234	7.1391	0.3536
24	3	84.2847	5.5410	3	77.9188	8.3290	6.3659	0.3322

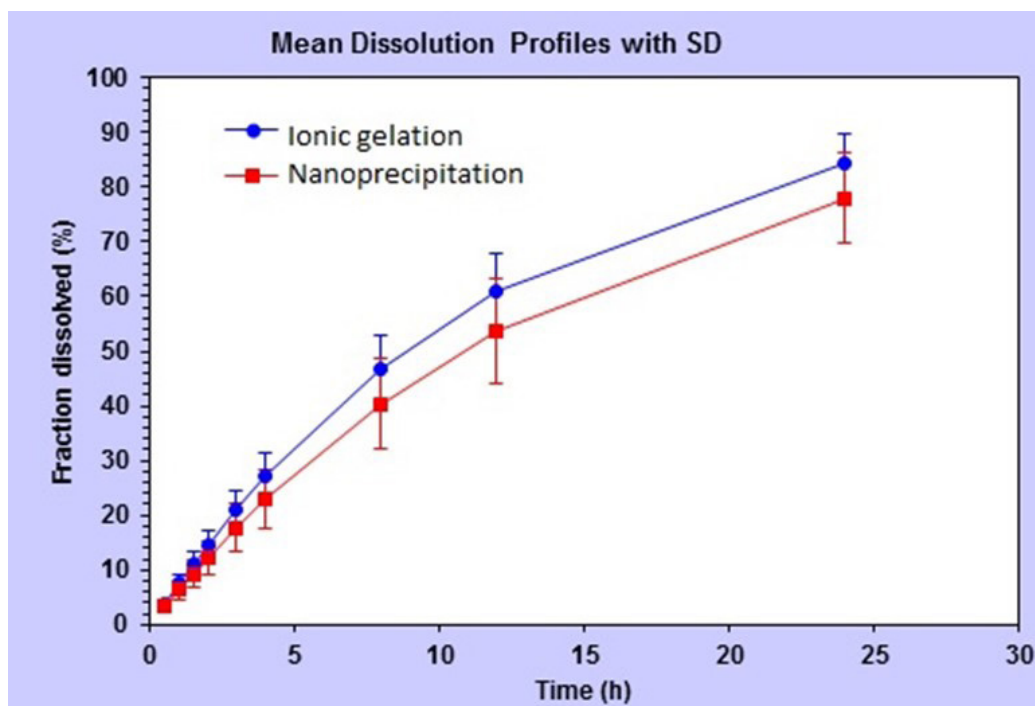


FIGURE 6 - Mean dissolution profile of Ionic gelation and Nanoprecipitation method.

CONCLUSION

The polysaccharide, Arabinoxylan from barley husks was extracted successfully having abundant features to be used in the formulation of novel drug delivery systems. The extracted AX was utilized as a polymer in the fabrication of DLP loaded NPs by ionic gelation and nanoprecipitation methods. Release profile and entrapment efficiency of NPs fabricated by Ionic gelation method were better as compared to Nanoprecipitation method. Furthermore, all the formulations displayed a sustained release profile over a period of 24 hours. FN1 prepared by ionic gelation method displayed maximum EE and drug release of about 79.59% and 82.55%, respectively among all formulations. Likewise, from the NP formulations prepared by nanoprecipitation method, FN4 displayed maximum EE and drug release of 63.76% and 78.58%, respectively. Hence, AX proved an excellent alternate over synthetic polymers for developing pH dependent controlled release nanocarrier system for acid labile drugs. This study concludes that barley husk is an economical source of biopolymers which can be employed in green polymer-based drug delivery systems having the potential for drug transport in a controlled manner.

FUNDING

The research received no external funding.

DISCLOSURE STATEMENT

The authors declare that they have no known competing financial interests or personal relationships that could have appeared to influence the work reported in this paper.

AUTHOR CONTRIBUTIONS

1. Ume Ruqia Tulain – Conceptualization, methodology, Administration and supervision
2. Alia Erum - Conceptualization, methodology, Administration and supervision
3. Nariman Shahid – Writing (original draft, revision and editing), Data analysis and validation.

4. Momina Usman - Investigation or data collection and writing original draft
5. Nadia Shamshad Malik – Methodology, Statistical analysis, supervision and validation
6. Amina Riaz - Writing (revision and editing)
7. Ayesha Rashid – Data analysis and validation
8. Sana Sajjad - Writing (revision and editing)

REFERENCES

- Ali U, Bijalwan V, Basu S, Kesarwani AK, Mazumder K. Effect of β -glucan-fatty acid esters on microstructure and physical properties of wheat straw arabinoxylan films. *Carbohydr Polym.* 2017;161:90-8.
- Ávila PF, Martins M, Goldbeck R. Enzymatic production of xylooligosaccharides from alkali-solubilized arabinoxylan from sugarcane straw and coffee husk. *BioEnergy Res.* 2021;14(3):739-51.
- Bansal K, Bajpai M. Formulation and evaluation of phanera variegata Linn. mucilage as a pharmaceutical binder in solid dosage form. *Indian J Pharm Educ Res.* 2020;54(4):971-82.
- Boddupalli BM, Ramani R, Anisetti B. Development and optimization of etoposide loaded nanoparticles by using DoE response surface central composite design. *Int J Bio-Pharma Res.* 2019;8(4):2531-40.
- Borjesson M, Hardelin L, Nylander F, Karlsson K, Larsson A, Westman G. Arabinoxylan and nanocellulose from a kilogram-scale extraction of barley husk. *BioResources.* 2018;13(3):6201-20.
- Bredenoord AJ, Pandolfino JE, Smout AJ. Gastro-oesophageal reflux disease. *Lancet.* 2013;381(9881):1933-42.
- Dadfar A, Edna T-H. Epidemiology of perforating peptic ulcer: A population-based retrospective study over 40 years. *World J Gastroenterol.* 2020;26(35):5302.
- Deng Y, Zhang X, Shen H, He Q, Wu Z, Liao W, et al. Application of the nano-drug delivery system in treatment of cardiovascular diseases. *Frontiers Bioeng Biotechnol.* 2020;7:489.
- Desu PK, Pasam V, Kotra V. Implications of superporous hydrogel composites-based gastroretentive drug delivery systems with improved biopharmaceutical performance of fluvastatin. *J Drug Delivery Sci Technol.* 2020;57:101668.
- Dhobale SM, Kolhe SS, Darekar PP, Dere TR, Date SH, Badhe PV. Extraction, characterization and evaluation of okara mucilage. *J Drug Delivery Ther.* 2019;9(3):325-8.

- Erum A, Tulain UR, Maqsood A, Malik NS, Rashid A, Warrach L, et al. Fabrication and comparative appraisal of natural and synthetic polymeric pH responsive nanoparticles for effective delivery of dexlansoprazole. *Polym Bull.* 2022;1-17.
- Erum A, Tulain UR, Maqsood A, Sidra, Malik NS, Rashid A, et al. Fabrication and comparative appraisal of natural and synthetic polymeric pH responsive nanoparticles for effective delivery of dexlansoprazole. *Polym Bull.* 2023;80(8):9113-29.
- Fujiwara Y, Arakawa T, Fass R. Gastroesophageal reflux disease and sleep. *Gastroenterol Clin.* 2013;42(1):57-70.
- Ganesh G, SaiKiran K, Satyanarayana VV, Karri R, Harris K, Baskaran M. Formulation and evaluation of dexlansoprazole delayed release capsules. *J Pharm Pharm.* 2016.
- Gaspar DP, Faria V, Gonçalves LM, Taboada P, Remunan-Lopez C, Almeida AJ. Rifabutin-loaded solid lipid nanoparticles for inhaled antitubercular therapy: Physicochemical and in vitro studies. *Int J Pharm.* 2016;497(1-2):199-209.
- Gaur N, Mishra S, Srivastava S, Parvez N. Naturapolyceutics-emerging science & technology in drug delivery system. *Int J Pharm Res.* 2020;(09752366).
- Gulia R, Singh S, Arora S, Sharma N. Development and optimization of hydrotropic solid dispersion of dexlansoprazole using central composite design approach. *J Integrated Sci Technol.* 2023;11(4):559.
- Guo R, Xu Z, Wu S, Li X, Li J, Hu H. Molecular properties and structural characterization of an alkaline extractable arabinoxylan from hull-less barley bran. *Carbohydr Polym.* 2019;218:250-60.
- Gupta S, Parvez N, Sharma PK. Extraction and characterization of hibiscus *rosasinensis* mucilage as pharmaceutical adjuvant. *World Appl Sci J.* 2015;33(1):136-41.
- Haseeb MT, Khaliq NU, Yuk SH, Hussain MA, Bashir S. Linseed polysaccharides based nanoparticles for controlled delivery of docetaxel: design, in vitro drug release and cellular uptake. *J Drug Delivery Sci Technol.* 2019;49:143-51.
- Jajere UM, Achadu A. Fabrication and characterization of ezetimibe solid dispersion for solubility enhancement. *Univers J Pharm Res.* 2017;2(1):11-4.
- Khan Y, Durrani S, Siddique M, Mehmood M. Hydrothermal synthesis of alpha Fe₂O₃ nanoparticles capped by Tween-80. *Mater Lett.* 2011;65(14):2224-7.
- Li C, Wang L, Chen Z, Li Y, Li J. Facile and green preparation of diverse arabinoxylan hydrogels from wheat bran by combining subcritical water and enzymatic crosslinking. *Carbohydr Polym.* 2020;241:116317.
- Moorthy IG, Maran JP, Ilakya S, Anitha S, Sabarima SP, Priya B. Ultrasound assisted extraction of pectin from waste artocarpus heterophyllus fruit peel. *Ultrason Sonochem.* 2017;34:525-30.
- Morales-Burgos A, Carvajal-Millan E, Sotelo-Cruz N, Rascon-Chu A, Lizardi-Mendoza J, Lopez-Franco Y. Highly cross-linked arabinoxylans microspheres as a microbiota-activated carrier for colon-specific insulin delivery. *Eur J Pharm Biopharm.* 2021;163:16-22.
- Nagarajana E, Shanmugasundarama P, Ravichandirana V, Vijayalakshmia A, Senthilnathanb B, Masilamanib K. Development and evaluation of chitosan based polymeric nanoparticles of an antiulcer drug lansoprazole. *J Appl Pharm Sci.* 2015;5(4):020-5.
- Nasiri MI, Yousuf RI, Shoaib MH, Siddiqui F, Qazi F, Ahmed K. Comparative pharmacokinetic evaluation of extended release itopride HCl pellets with once daily tablet formulation in healthy human subjects: a two treatment, four period crossover study in fasted and fed condition. *Drug Dev Ind Pharm.* 2019;45(3):415-22.
- Ngwuluka NC. Responsive polysaccharides and polysaccharides-based nanoparticles for drug delivery. *Stimuli Responsive Polym Nanocarriers Drug Delivery Appl.* 2018;1: 531-54.
- Raval N, Maheshwari R, Kalyane D, Youngren-Ortiz SR, Chougule MB, Tekade RK. Importance of physicochemical characterization of nanoparticles in pharmaceutical product development. *Basic Fundam Drug Deliv.* 2019;1:369-400.
- Roos AA, Persson T, Krawczyk H, Zacchi G, Stalbrand H. Extraction of water-soluble hemicelluloses from barley husks. *Bioresour Technol.* 2009;100(2):763-9.
- Shahid N, Erum A, Zaman M, Iqbal MO, Riaz R, Tulain R, et al. Fabrication of thiolated chitosan based biodegradable nanoparticles of ticagrelor and their pharmacokinetics. *Polym Polym Compos.* 2022;30:09673911221108742.
- Sharma N, Madan P, Lin S. Effect of process and formulation variables on the preparation of parenteral paclitaxel-loaded biodegradable polymeric nanoparticles: A co-surfactant study. *Asian J Pharm Sci.* 2016;11(3):404-16.
- Shrestha UR, Smith S, Pingali SV, Yang H, Zahran M, Breunig L, et al. Arabinose substitution effect on xylan rigidity and self-aggregation. *Cellulose.* 2019;26(4):2267-78.
- Sontale R, Koshta A, Muley P, Malviya S, Kharia A. Formulation and Evaluation of dexlansoprazole floating tablets. *Int J Pharm Life Sci.* 2020;11(1).
- Tulain UR, Mahmood A, Aslam S, Erum A, Shamshad Malik N, Rashid A, et al. Formulation and evaluation of Linum

usitatissimum mucilage-based nanoparticles for effective delivery of ezetimibe. *Int J Nanomed.* 2021;4579-96.

Wan D, Zhao M, Zhang J, Luan L. Development and in vitro-in vivo evaluation of a novel sustained-release loxoprofen pellet with double coating layer. *Pharmaceutics.* 2019;11(6):260.

Wikiera A, Mika M, Grabacka M. Multicatalytic enzyme preparations as effective alternative to acid in pectin extraction. *Food Hydrocolloids.* 2015;44:156-61.

Zaman M, Hanif M, Khan MA. Arabinoxylan-based mucoadhesive oral films of tizanidine HCL designed and optimized using central composite rotatable design. *Polym-Plast Technol Eng.* 2018;57(5):471-83.

Received for publication on 14th November 2023

Accepted for publication on 19th March 2024